submitted to Scripta Materialia

The Stability of Lomer-Cottrell Jogs in Nanopillars

Christopher R. Weinberger[a,*], Wei Cai[b]

[a] *Sandia National Laboratories, P.O. Box 5800, MS1411, Albuquerque NM, 87185-1411*
[b] *Department of Mechanical Engineering, Stanford University, CA 94305-4040*

Abstract

Single arm spiral sources, or truncated Frank-Read sources, have been used frequently to interpret the size dependent plasticity in micropillars. The basis for these sources is strong pinning points which have been proposed to exist based on immobile Lomer-Cottrell jogs. Here, we show using molecular dynamics of FCC nanopillars that Lomer-Cottrell jogs are not as immobile as initially thought and that they do not provide strong pinning points for single arm sources.

Keywords: dislocations, micropillar, jog

Experiments on pillars ranging in sizes from a few hundred nanometers to tens of micrometers have shown that the flow stress in the pillars increases as pillar size decreases [1, 2, 3]. The plastic deformation of these pillars must occur through the activation of dislocation sources which increase in strength as the pillar diameter decreases. Two competing mechanisms have emerged to explain the experimental observations: dislocation starvation [4] and single arm sources [5]. The dislocation starvation model maintains that mobile dislocations escape the crystals leaving them starved of mobile dislocations and plasticity continues with nucleation from the surface. The single arm source model claims that truncated Frank-Read sources control plasticity and the strengthening is caused by shorter source lengths in smaller volumes. However, this model requires strong pinning points and the nature of these pinning points is unclear.

The single arm source model is primarily supported by dislocation dynamics (DD) simulations [6, 7] and some experiments [8]. These DD simulations require strong pinning points that are created by dislocation segments or junctions which are assumed to be immobile. In order to provide a theoretical basis for single arm sources, Lee and Nix [9] investigated the creation of strong pinning points from Lomer-Cottrell (LC) junctions in FCC micropillars. They conclude that LC junctions can indeed form single arm sources by transforming into LC jogs but rely on the immobility of the jog. In this letter, we investigate the stability and mobility of LC jogs and evaluate their potential as single arm sources.

Here, we will distinguish between Lomer dislocations, which are perfect dislocations, and Lomer-Cottrell dislocations which are the dissociated form of a Lomer dislocation involving a stair-rod dislocation at the line of intersection and two Shockley partials on different $\{111\}$ planes. Both types of dislocations can be formed by the reaction of two glissile dislocations on different $\{111\}$ planes that result in an edge dislocation whose glide plane is $\{001\}$. For example, the reaction $\frac{a}{2}[101](1\bar{1}1) + \frac{a}{2}[01\bar{1}](111) = \frac{a}{2}[110](001)$ is energetically favorable to form a Lomer lock. The Lomer dislocation is often considered immobile because its glide plane is $\{001\}$, which is not a close packed plane in an FCC crystal, and the Lomer-Cottrell dislocation is immobile because it

*Corresponding author
Email addresses: crweinb@sandia.gov (Christopher R. Weinberger), caiwei@stanford.edu (Wei Cai)

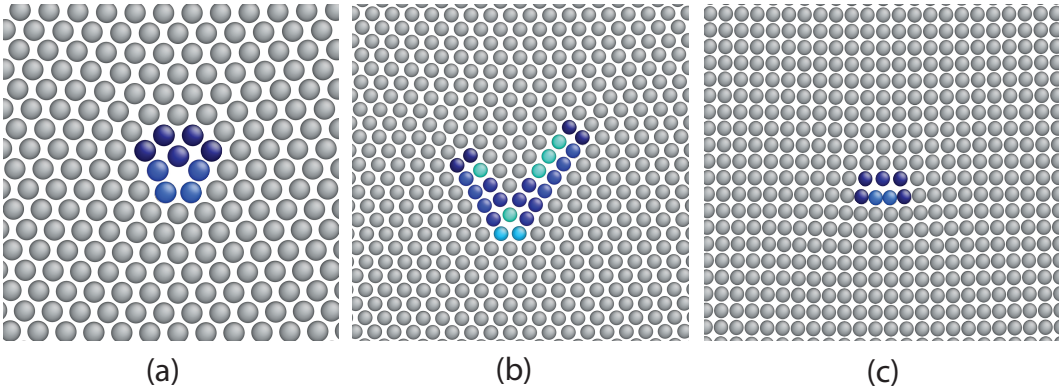

Figure 1: (color) The dislocation core for (a) a Lomer dislocation, (b) a Lomer-Cottrell Lock, and (c) a 45° mixed dislocation on a {100} plane. The atoms are colored by centro-symmetry deviation parameter [10] and the material shown here is copper.

is an extended dislocation on two different planes. It is generally believed that the Lomer-Cottrell dislocation should be the naturally occurring core structure of the dislocation because, according to elasticity theory, it should have a lower energy. However it has been shown using HRTEM [11] that dislocations with this character will form compact cores in aluminum subgrain boundaries, which is supported by EAM models of these materials [12]. To ascertain the mobility of these types of dislocations, we have conducted quasi-static (zero Kelvin) simulations of the core structure of these types of dislocations for nickel and copper. Periodic boundary conditions (PBC) are applied along the dislocation line. Our simulations show that the compact core and dissociated core of a $\langle 110 \rangle \{001\}$ edge dislocation are both metastable. In both materials studied here, if the dislocation is created using the displacement field of a perfect edge dislocation, the relaxed core structure is the compact type shown in Figure 1(a). When we attempt to compute the Peierls stress, the Lomer dislocations emit Shockley partials from their cores when very high shear stresses are applied (greater than 1 GPa). The dissociated cores do not move either, but the applied stress does affect the intrinsic stacking fault size asymmetrically, causing one to grow and the other to shrink while the stair-rod remains immobile for stresses greater than 1 GPa. Thus, these types of dislocations should be highly immobile in the bulk regardless of which core structure is realized. However, LC jogs, which are the subject of investigation in this letter, are different from the Lomer and LC dislocations because it has two end nodes, one of which is always constricted [9], about which the dislocation arms can rotate.

To investigate the stability of LC jogs, we use molecular dynamics simulations. This is done by introducing a jog into a dislocation that spans a nanopillar as shown in Figure 2(a). Most of the nanopillars in our simulations have a diameter of 16 and 30 nm, while a few have a diameter of 50 nm. The pillars have free side surfaces and have a circular cross-section with PBC along their length. The jog length in most of the simulations is $15\frac{a}{2}\langle 110 \rangle$, however doubling the jog length in 30 nm diameter pillars showed no significant change in the jog behavior. Two different orientations are studied, $\langle 100 \rangle$ and $\langle 111 \rangle$. The $\langle 100 \rangle$ nanopillars are loaded with a compressive stress along their axis while the $\langle 111 \rangle$ are loaded by applying a shear stress to the pillar. The stability of the LC jog is studied under both constant stress (0 MPa, 500 MPa and 1 GPa) and constant strain (0% and 3%) and at 300 K as well as 0 K except for the 50 nm pillars, which we only study at 300 K and 1 GPa. The effect of stacking fault energy is included in the study using the Foiles-Hoyt [13] potential for nickel and Mishin [14] potential for copper.

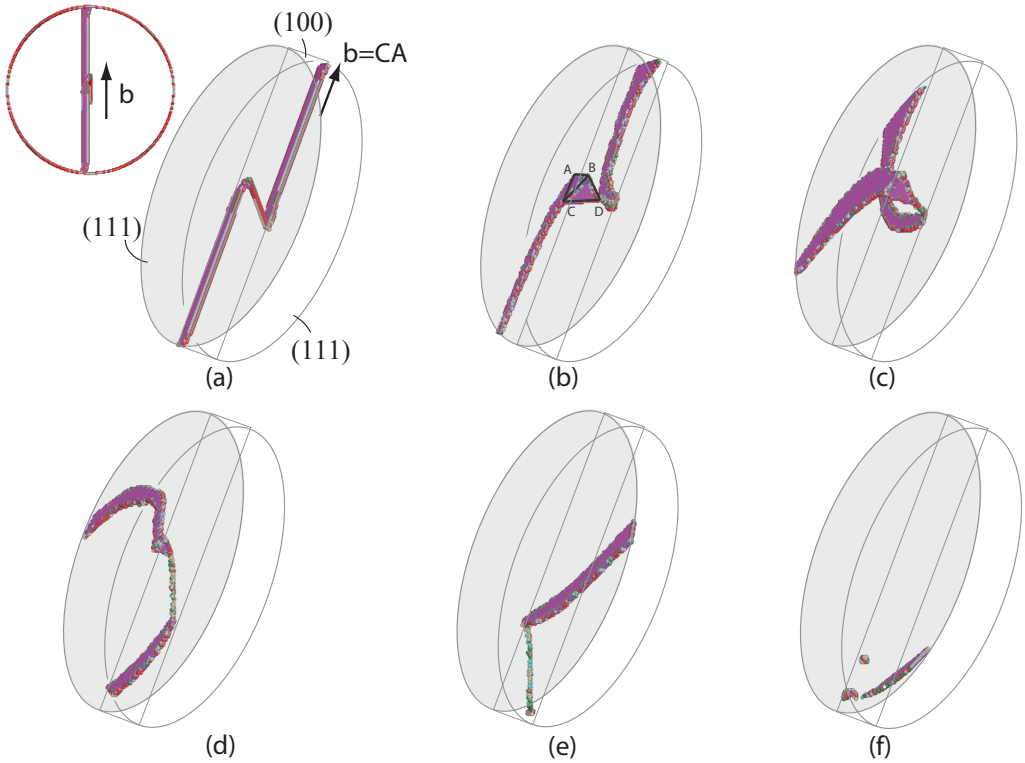

Figure 2: The operation of a single arm source created from a Lomer-Cottrell jog and its dissolution in a 30 nm diameter nickel nanopillar with a jog length of $30\frac{a}{2}\langle 110\rangle$. (a) The initial configuration of the source showing both an end on view of the pillar with surface atoms present and a perspective view of the initial source at 0 picoseconds. (b) The extended node readily forms as predicted from geometrical considerations at 4 piscoseconds. (c) The arms rotate past each other on their $\{111\}$ planes at 10 picoseconds. The jog rotates on its $\{100\}$ plane eliminating the extended node and forming a constricted jog along the whole jog length (d) (18 picoseconds). (e) The dislocation structure drifts along the $\{100\}$ plane at 40 picoseconds and (f) eventually leaves the nanopillar at 48 picoseconds. Movies of this simulation can be found on the web in the supplemental information.

For $\langle 100 \rangle$ oriented nanopillars, two basic behaviors are observed which is determined by the magnitude of the applied load. If the applied axial load is above a critical stress, the dislocation is able to escape when the arms rotate and constrict the nodes of the LC jog allowing the jog to rotate on its glide plane as shown in Figure 2. The initial condition is a screw dislocation dissociated on a $\{111\}$ plane with a LC jog connecting the two arms as shown in Figure 2(a). Under the applied axial load (1GPa here), we see the arms begin to rotate (Figure 2(b)). One node of the LC jog is extended and the other is constricted, Figure 2(b), similar to that predicted by Lee and Nix [9]. However, at this point the constriction has already spread partway along the jog. As the arms continue to rotate, Figure 2(c)-(d), we see that the LC jog changes to a constricted core eliminating the extended node, Figure 2(d)-(e) . Lee and Nix predicted a dissociated core structure with constrictions at both ends, but here we observe that the core is constricted along its whole length. If the arms were to rotate 180° of this configuration, the extended core structure often does not return (as is observed in other simulations), but rather the jog would remain constricted. This is because the Lomer dislocation is apparently able to rotate on its $\{100\}$ glide plane out of the edge configuration. The new orientation does not intersect $\{111\}$ planes preventing dissociation onto $\{111\}$ type planes. The dislocation is able to freely move along the $\{100\}$ plane as shown in Figure 2(e) to which the jog is confined, and eventually the jog escapes as shown in Figure 2(f). The rotation and constriction of the LC jog, which facilitate escape, are features observed in all of our simulations illustrating the mobility of these dislocation structures.

If the applied stress is below the activation stress of the source, the dislocation immediately reorients itself eliminating the LC jog. The LC dislocation again begins to rotate on the $\{100\}$ plane while extending its length and reducing the length of the dissociated screw dislocations. The driving force for the reorientation is line tension since the energy of the dislocation can be reduced by reducing its total line length through the lengthening of the jog. In some cases, the dislocation is able to escape in the short simulation time. In all the simulations the LC jog is able to rotate in its $\{100\}$ plane, illustrating that the reorientation of the jog is not an artifact of the high stresses in the previous simulations. Similar to the high stress cases, the reorientation and loss of the strong pinning points originates from the ability of the LC jog to reorient from its edge orientation to a mixed dislocation on the $\{100\}$ plane.

Additional simulations were performed for $\langle 111 \rangle$ oriented nanopillars to ensure the generality of the observed behavior. In this case, the dislocation arms that should act as single arm sources are oriented perpendicular to the pillar axis. Thus, as the arms rotate their line length does not change significantly which may, perhaps, increase their stability. Similar to the $\langle 100 \rangle$ orientation, simulations at 300 K and 0 K under constant stress and strain were performed. However, despite the geometry changes, the behavior is quite similar to what was observed in $\{100\}$ pillars. The results for a 30 nm nickel pillar at 300 K and zero applied stress is shown in Figure 3. The behavior is typical for the low stress simulations. The initial condition shows the pillar with two screw dislocation arms and an LC jog, Figure 3(a). The jog begins to reorient, Figure 3(b), by rotating in the $\{100\}$ plane as it consumes one of the arms. The arm that is consumed was originally connected to the constricted node, as the extended node is clearly shown in the Figure. Finally, we see that the $\{100\}$ dislocation is now stretched over most of the pillar, thus reducing its line energy and eliminating its potential as a single arm source. At high stresses, the jog loss is similar to the $\langle 100 \rangle$ orientation.

To further understand the mobility of dislocations on $\{100\}$ planes in FCC crystals, we performed quasi-static calculations of the Peierls stress and core structure of 45° mixed dislocations. Since the edge dislocations, or Lomer and Lomer-Cottrell dislocations, have non-planar cores and high Peierls stresses and screw dislocations should dissociate onto $\{111\}$ planes and become highly mobile, we use the 45° mixed dislocation as a test case for mobility of mixed dislocations on $\{100\}$

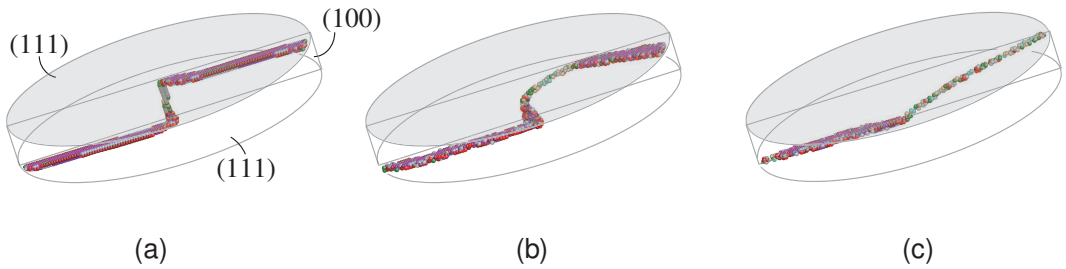

Figure 3: The dissolution of a LC jog in a {111} oriented 30 nm diameter nickel nanopillar under zero applied stress. (a) The initial jog structure where the arms are perpendicular to the pillar axis. (b) The constricted node extends the dislocation on the {100} plane, reorienting the dislocation away from edge under line tension forces at 3 picoseconds. (c) The {100} dislocation has extended all the way to the free surface effectively eliminating the jog at 9 picoseconds. Movies of this simulation can be found on the web in the supplemental information.

planes. The core structure of these dislocations is shown in Figure 1(c), which is planar in nature. This suggests that mixed dislocations on the {100} should be significantly more mobile than edge dislocations. The Peierls stress of the two different metals is 145 MPa and 65 MPa for nickel and copper respectively. We note that these values are significantly lower than those obtained for dislocations oriented in the LC direction. Thus, once the dislocation is able to rotate out of the LC orientation, it is able to glide allowing the LC jog to dissolve.

These molecular dynamics simulations show that LC jogs are more mobile than initially thought. None of our simulations show a stable single arm source. These jogs are unstable in nanopillars when the arms begin to rotate, which suggests they are unable to provide strong pinning points in micro- and submicrometer pillars. The origin of strong pinning points that create single arm sources is unclear. It is possible that impurities may segregate to dislocation cores and pin the dislocations, which may explain the observations of single arm sources observed in some experiments [8]. However, from these results it is doubtful that dislocation structures such as LC jogs are strong enough to create the necessary pinning points and permanent dislocation sources. These results also point to the necessity of performing additional molecular dynamics studies on the stability of dislocation structures that may give rise to single arm sources.

Acknowledgement

This research was supported in part by an appointment to the Sandia National Laboratories Truman Fellowship in National Security Science and Engineering, sponsored by Sandia Corporation (a wholly owned subsidiary of Lockheed Martin Corporation) as Operator of Sandia National Laboratories under its U.S. Department of Energy Contract No. DE-AC04-94AL85000. The work was partly supported by National Science Foundation Career Grant CMS-0547681 and the Army High Performance Computing Research Center at Stanford.

Bibliography

[1] Uchic, M., Dimiduk, D., Florando, J. & Nix, W. Sample dimensions influence strength and crystal plasticity. *Science* **305**, 986–989 (2004).

[2] Greer, J. R., Oliver, W. C. & Nix, W. D. Size dependence of mechanical properties of gold at the micron scale in the absence of strain gradients. *Acta Materialia* **52**, 1821–1830 (2005).

[3] Dimiduk, D., Uchic, M. & T.A.Parthasarathy. Size-affected single-slip behavior of pure nickel microcrystals. *Acta Materialia* **53**, 4065–4077 (2005).

[4] Greer, J. & Nix, W. Nanoscale gold pillars strengthened through dislocation starvation. *Phys. Rev. B* **73**, 245410 (2006).

[5] Rao, S. *et al.* Athermal mechanisms of size-dependent crystal flow gleaned from three-dimensional discrete dislocation simulations. *Acta Materialia* **56**, 3245–3259 (2008).

[6] Tang, H., Schwarz, K. & Espinosa, H. Dislocation-source shutdown and the plastic behavior of single-crystal micropillars. *Phys. Rev. Lett.* **100**, 185503 (2008).

[7] Motz, C., Weygand, D., Senger, J. & Gumbsch, P. Initial dislocation structures in 3-d discrete dislocation dynamics and their influence on microscale plasticity. *Acta Mater.* **57**, 1744–1754 (2009).

[8] Oh, S., Legros, M., Kiener, D., Gruber, P. & Dehm, G. In situ TEM straining of single crystal Au films on polyimide: Change of deformation mechanisms at the nanoscale. *Acta Mater.* **55**, 5578 (2007).

[9] Lee, S.-W. & Nix, W. D. Geometrical analysis of 3d dislocation dynamics simulations of fcc micro-pillar plasticity. *Mater. Eng. Sci A* **527**, 1903–1910 (2010).

[10] Kelchner, C. L., Plimpton, S. J. & Hamilton, J. C. Dislocation nucletation and defect structure during surface indentation. *Phys. Rev. B* **58**, 11085–11088 (1998).

[11] Mills, M. J. & Stadelman, P. A study of the structure of Lomer and 60° dislocations in aluminum using high-resolution transmission electron microscopy. *Philos. Mag.* **60**, 355–384 (1989).

[12] Mills, M. J., Daw, M. S. & Foiles, S. M. High-resolution transmission electron microscopy studies of dislocation cores in metals and intermetallic compounds. *Ultramicroscopy* **56**, 79–93 (1994).

[13] Foiles, S. M. & Hoyt, J. J. Computation of grain boundary stiffness and mobility from boundary fluctuations. *Acta Mater.* **54**, 3351–3357 (2006).

[14] Mishin, Y., Mehl, M., Papaconstantopoulos, D., Voter, A. & Kress, J. Structural stability and lattice defects in copper: Ab initio, tight-binding, and embedded-atom calculations. *Phys. Rev. B* **63**, 224106 (2001).

1. Supplemental Information

Movie 1: A movie showing the escape of the LC jog shown in Figure 2. Some of the surface atoms are removed to provide a perspective view of escape mechanism

Movie 2: An alternative view of Movie 1.

Movie 3: A movie showing the escape of the LC jog shown in Figure 3. Some of the surface atoms are removed to provide a perspective view of escape mechanism

Movie 4: An alternative view of Movie 3.